Energy & Environmental Science

Cite this: *Energy Environ. Sci.*, 2012, **5**, 7368

www.rsc.org/ees

PAPER

Efficient CO_2 sorbents based on silica foam with ultra-large mesopores†

Genggeng Qi, Liling Fu, Brian Hyun Choi and Emmanuel P. Giannelis*

Received 16th February 2012, Accepted 19th March 2012
DOI: 10.1039/c2ee21394j

A series of high-capacity, amine impregnated sorbents based on a cost-effective silica foam with ultra-large mesopores is reported. The sorbents exhibit fast CO_2 capture kinetics, high adsorption capacity (of up to 5.8 mmol g^{-1} under 1 atm of dry CO_2), as well as good stability over multiple adsorption–desorption cycles. A simple theoretical analysis is provided relating the support structure to sorbent performance.

Introduction

Rising levels of atmospheric CO_2 from the consumption of fossil fuels have been widely implicated to be a main contributor to global climate change.[1] Post-combustion capture from existing power plants provides a viable near-term solution from surging CO_2 emissions. The current state-of-the-art industrial process for post-combustion capture—amine scrubbing—is based on CO_2 absorption using aqueous amine solutions or chilled ammonia, which suffers from relatively low energy efficiency and issues associated with the use of liquid amine solvents such as equipment corrosion, solvent loss, and toxicity. To overcome such challenges, adsorption *via* solid-supported amines has been proposed as an attractive alternative for low temperature post-combustion capture. Solid-supported amines are highly selective towards CO_2 and their capture capacity is much more robust in the presence of moisture compared to sorbents based mainly on physisorption, such as zeolites, activated carbons, many metal–organic frameworks and porous polymers.[2–5] Meanwhile, the disadvantages associated with sorbent regeneration and corrosiveness can potentially be reduced as amines are anchored to a solid support.

Because of their attractive properties such as large surface area, tunable pore structure, and high thermal stability, mesoporous silicas are considered promising supports for amine immobilization. A series of solid-supported amine sorbents, based on bulk mesoporous silica including MCM-41, MCM-48, SBA-12, SBA-15, SBA-16, and KIT-6, has been prepared *via* wet impregnation and evaluated.[6–15] They show fast CO_2 adsorption kinetics and enhanced capacity compared to those based on aqueous amine solutions, *e.g.* ~1.25 mmol g^{-1} for 30% monoethanolamine (MEA) solution.[16] However, the highest capture capacities of the solid sorbents were about 4 mmol g^{-1} under 1 atm dry CO_2, barely above the capacity threshold to economically compete with the amine-scrubbing process.[17] It has been demonstrated that the structure of the supports play a crucial role in sorbent performance. In general, large pore size and good pore interconnection tend to improve sorbent capacity.[7,11,18–20] To that end, significant efforts have been directed towards developing supports with optimized structures in order to further improve the performance of sorbents. Mesocellular foams,[21–23] mesoporous silica with textural (interparticular) mesoporosity,[24] and hierarchical monoliths[25] appear more efficient than related bulk mesoporous silica supports. Recently, we reported a family

Department of Materials Science and Engineering, Cornell University, Ithaca, NY 14853, USA. E-mail: epg2@cornell.edu

† Electronic supplementary information (ESI) available: XRD patterns and ATR/FTIR spectra of supports and sorbents, sorbent weight-loss, sorbent deactivation comparison, the sorbent capacities using the recycled foams, and the model about the relationship between the structure of bulk mesoporous supports and sorbent performance. See DOI: 10.1039/c2ee21394j

Broader context

Increases in atmospheric carbon dioxide have been implicated as one of the main causes of global climate change. Post-combustion capture shows the greatest near-term potential for reducing CO_2 emissions. Adsorption using supported amine sorbents provides a promising alternative to conventional amine scrubbing. However, CO_2 capture in practical applications has been impeded primarily by limited sorbent capacity and recyclability, and relatively high sorbent cost. Here we present a series of high-capacity amine sorbents supported on a cost-effective silica foam with ultra-large mesopores. The sorbents exhibit fast CO_2 capture kinetics, high adsorption capacity, as well as good stability over multiple adsorption–desorption cycles. A theoretical analysis is provided for the first time relating the support structure to sorbent performance, which may direct the structural optimization of sorbent supports.

of sorbents based on hollow mesoporous silica spheres with well-defined sizes and shell thicknesses.[26] Impregnated with tetraethylenepentamine, the sorbents exhibit outstanding capacities up to 6.7 mmol g^{-1} under 1 atm dry CO_2.[27] However, most of these advanced supports are not cost-effective. Their synthesis is generally performed under strong acidic or basic conditions using relatively expensive tetraalkoxysilanes as silica precursors. Additives, such as micelle swelling agents, porogens and hard templates and/or post-pore-expansion treatment is necessary to generate larger mesopores and hierarchical structures.

Herein we report a family of high-efficiency supported amine sorbents based on a more cost-effective silica foam with ultra-large mesopores. The new sorbent support was synthesized from an inexpensive silica source, sodium silicate, under nearly neutral conditions. No micelle swelling agents, *e.g.* 1,3,5-trimethylbenzene, are required in the synthesis, which may significantly simplify the scale-up synthesis and reduce cost. The sorbents exhibit fast CO_2 adsorption–desorption kinetics, outstanding working capacity, as well as good stability over multiple adsorption–desorption cycles. Moreover, the sorbents exhibit relatively low reaction heat compared to amine-scrubbing solvents such as 30% MEA solution leading to less energy penalty for sorbent regeneration. Furthermore, the relationship between support structure and sorbent performance was investigated. A theoretical model, described here for the first time, provides further insights and can guide the design of optimized sorbents.

Experimental

Chemicals

Triblock copolymer poly(ethylene oxide)-*b*-poly(propylene oxide)-*b*-poly(ethylene oxide) surfactant P123 ($EO_{20}PO_{70}EO_{20}$, $M_v = 5800$), sodium silicate, acetic acid, ammonium fluoride, polyethylenimines (PEI423, $M_n \approx 423$ with 5–20% tetraethylenepentamine, and PEI10k, $M_n \approx 10\,000$), glycerol diglycidyl ether (GDE) and ethanol (v/v = 90%) were purchased from Aldrich and used without further purification unless otherwise stated. Deionized water was generated with a Milli-Q integral pure and ultrapure water purification system and used in all experiments.

Sorbent supports

The foam support was prepared as follows: 3.0 g of P123 was dissolved in a solution of acetic acid (3.0 g), water (52 g), and ammonium fluoride (0.3 g) at 40 °C. A solution of sodium silicate (2.35 g) in water (40 g) was heated to 40 °C and poured into the surfactant solution under vigorous stirring. The mixture was kept under static conditions at 40 °C for 24 h and aged at 70 °C for another 24 h. The product was collected by filtration, followed by copiously washing with DI water. The surfactant P123 was removed by calcination at 560 °C for 6 h. The synthesis of the foam is readily scalable. For example, we have succeeded in developing a pilot process to produce the foam in kilogram amounts, details of which will be published elsewhere.

To investigate the stability of the support, 0.1 g of the foam was dispersed in 4 ml of DI water and continuously sonicated for 2 h using a Branson 3510-DTH ultrasonic cleaner. The treated foam was then characterized by transmission electron microscopy (TEM). To assess its chemical stability and reusability, 0.25 g of the foam was loaded with 1 g of PEI423 and kept at 75 °C in the air for 24 h. The impregnated amine was then removed from the foam by copiously washing with ethanol and the foam was collected by centrifugation. The amine impregnation-removal process was repeated 5 times during which a small fraction of the sorbent with an 80 wt% amine loading was taken to measure the capacity. Furthermore, the stability of the foam under harsh conditions was assessed by performing a steam treatment according to a previously published procedure.[28] A 4 ml glass vial containing 0.3 g of the foam was put into a 20 ml glass vial that was filled with 10 ml of DI water. The vials were then sealed in a 100 ml Teflon-lined laboratory autoclave from Parr Instruments. The autoclave was heated to 106 °C and kept at that temperature for 30 h. The obtained silica foam sample was dried under 0.02 mbar at 25 °C for 24 h and stored in a desiccator.

To study the effect of support structure on sorbent performance, in addition to the silica foam, two controls, bulk mesoporous silica SBA-15 and MCM-41, were synthesized following previous reports.[27,29]

Sorbent preparation

Sorbents based on the mesoporous foam, denoted as F-PEI*x*%*y* where *x* represents the number average molecular weight of the amine and *y* stands for the weight percentage of PEI in the sorbent, were prepared *via* wet impregnation using 10 wt% PEI ethanol solution.[6,27] In a typical preparation, a given amount of 10 wt% PEI ethanol solution was added to 40 mg of the silica foam. The mixture was then stirred at room temperature for 30 min and kept under 70 mbar at 40 °C for 24 h. The sorbent was further dried under 0.02 mbar at 25 °C for 24 h and stored in a desiccator before further measurements. Sorbents based on bulk mesoporous silicas SBA-15 and MCM-41 were synthesized in the same manner and denoted as SBA-15-PEI423%*y* and MCM-41-PEI423%*y*, in which *y* represents the PEI loading of the sorbents.

CO_2 adsorption and regeneration of sorbents

CO_2 adsorption–desorption measurements shown schematically in Fig. 1 were performed using a TA Instruments Q500 thermal graphic analyzer. 1 atm of dry CO_2 balanced with N_2 was used for the adsorption runs and ultra high purity N_2 (99.995%) was used as the purging gas for sorbent regeneration. In a typical

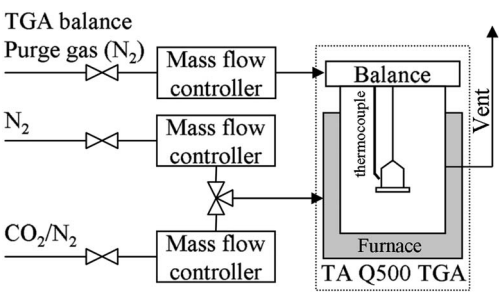

Fig. 1 Schematic representation of the experimental setup for CO_2 adsorption and desorption studies.

adsorption process, about 5–10 mg of F-PEI423%80 was placed in a platinum sample pan. After being heated to 100 °C in a stream of N_2 (~40 ml min^{-1}) and held at that temperature for 40 min to remove any moisture and CO_2 adsorbed from the air, the sorbent was cooled down to 75 °C at a rate of 10 °C min^{-1} and equilibrated at that temperature for 30 min. The gas was then switched to 1 atm 80% dry CO_2 balanced with N_2 (~40 ml min^{-1}) for 60 min at 75 °C. The CO_2 capacity of the sorbents in mmol g^{-1} was calculated based on the weight gain of the sorbent during the adsorption. After the adsorption step the gas was switched back to N_2 and the sorbent was regenerated at 75 °C.

In the cyclic adsorption–desorption tests, the sorbents were activated as described above at 100 °C for 40 min in N_2 (~40 ml min^{-1}). The sorbent was cooled down to 75 °C at a rate of 10 °C min^{-1} and equilibrated at that temperature for 30 min. The gas was then switched to 80% CO_2 (~40 ml min^{-1}) for 10 min at 75 °C for the adsorption study. In the temperature swing process, the sorbent was heated to 100 °C at a rate of 10 °C min^{-1} and held at that temperature for 5 min in N_2. In the concentration sweep process, the sorbent was regenerated in N_2 at 75 °C for 30 min. The adsorption–desorption procedure was repeated for 100 cycles to evaluate the long-term stability of the sorbents.

Characterization

X-ray diffraction (XRD) patterns of the silica foam were recorded on a Rigaku SmartLab X-Ray diffractometer using Cu Kα radiation ($\lambda = 0.1541$ nm). Attenuated total reflectance/Fourier transform infrared (ATR/FTIR) spectra were collected on a Nicolet iZ10 FT-IR spectrometer with 4 cm^{-1} resolution at room temperature. TEM analysis was conducted by a FEI TECNAI T12 Twin transmission electron microscope, operated at 120 kV. Mesoporous silica samples were prepared by placing a droplet of ethanol-diluted silica dispersion on a formvar/carbon coated microscope grid and dried in air. As sorbents based on bulk MCM-41 and SBA-15 are gel-like at high PEI loadings, to investigate their morphology, a given amount of freshly prepared PEI423 and GDE (v/v = 1 : 1) ethanol solution (21.4 wt%) was impregnated into these silica supports and crosslinked following the reported method.[27] The derived composites, denoted as MCM-41PEI423-GDE%*m* and SBA-15PEI423-GDE%*m* where *m* is the polymer loading in the composites equivalent to *y* in SBA-15-PEI423%*y* and MCM-41-PEI423%*y*, were cut by a Leica UC7 cryomicrotome into 100 nm slices at −60 °C and loaded onto carbon coated copper microgrids *via* dry pickup. For F-PEI423%83, a small amount of the sticky powder was spread on a formvar/carbon coated microscope grid with a laboratory spatula for TEM characterization. Nitrogen physisorption isotherms were measured at 77 K using a Micromeritics ASAP 2020 analyzer. The silica supports were degassed at 423 K under vacuum for 24 h, while the sorbents were degassed at 323 K under vacuum for 24 h. The specific surface areas of the supports and the sorbents were calculated by the Brunauer–Emmett–Teller (BET) method. The total pore volume was estimated from the amount of N_2 adsorbed at a relative pressure of 0.99. The pore size and the size distribution of the foam and the foam-supported PEI sorbents were calculated using the simplified Broekhoff–de Boer method,[30] while those of MCM-41, SBA-15 and their sorbents were estimated by the Barrett–Joyner–Halenda (BJH) model. The enthalpy changes during CO_2 adsorption and sorbent regeneration were estimated using a TA Q2000 differential scanning calorimeter (DSC) following the reported method.[17] The DSC was calibrated for temperature using the melting point of indium and the heat capacity using a sapphire crystal. In a typical measurement, about 6 mg of F-PEI423%80 was loaded in a Tzero aluminium pan and covered with a pan lid having a pinhole (~1 mm in diameter). The sample was heated from 40 to 100 °C and activated in pure nitrogen (50 ml min^{-1}) for 20 min. The sample was then cooled down to 40 °C and held isothermally for 10 min. After that, the sample was heated to 75 °C at a rate of 10 °C min^{-1} and equilibrated at 75 °C for 30 min. Subsequently, the gas was switched from N_2 to pure CO_2 and maintained at 75 °C for 60 min, after which the gas was switched back to N_2 and held at 75 °C for another 60 min. The apparent heat change caused by the gas switch was corrected using an empty Tzero aluminium pan with a pan lid. Three freshly prepared sorbent samples were replicated to minimize the measurement error. The adsorption heat, the desorption heat and the sensible heat of the sorbent were calculated by integrating the heat flow during the adsorption step, the desorption step and the temperature ramping step from 100–40 °C, respectively.

Results and discussion

Characterization of sorbents

The structure and morphology of the supports and amine supported sorbents were investigated *via* TEM. As shown in Fig. 2a, the units of the foam are interconnected cells. Even without the use of any micelle swelling agents, these cells are considerably larger (~50 to 120 nm) with a broad size distribution compared to mesocellular foams (with cell sizes typically <50 nm) prepared under either strong acidic conditions[31] or in a nearly neutral emulsion (MSU-F).[32] In an attempt to evaluate its mechanical robustness the foam was sonicated in water for two hours. No significant structural changes could be seen in Fig. 2b suggesting that the foams are fairly robust under these conditions. Furthermore, no discernible changes were observed after the foam was subjected to treatment with steam at 106 °C for 30 h (Fig. 2c). The TEM images of mesoporous silica MCM-41 and SBA-15 supports are shown in Fig. 2d and e. Fig. 2f and g compare the structure of the foam-supported amine sorbent with those based on MCM-41 and SBA-15. These images suggest that the amine is distributed in a relatively uniform coating on and inside the foam. In contrast, a substantial amount of the polymer (the white/grey areas in the TEM images) is on or between particles in the MCM-41 and SBA-15 based sorbents.

The structural properties of the foam and its derived sorbents were also analyzed by means of nitrogen physisorption and X-ray diffraction. For the as-synthesized foam, a type IV N_2 adsorption isotherm with pronounced capillary condensation starting at $P/P^0 \approx 0.7$ was obtained (Fig. 3). The BET surface area and the total pore volume of the foam are 446 m^2 g^{-1} and 1.46 cm^3 g^{-1}, respectively. The pore size distribution of the foam is bimodal, with a small peak between 10 and 20 nm and another broad peak corresponding to pores with a size larger than 40 nm. The BET surface area and the total pore volume of the

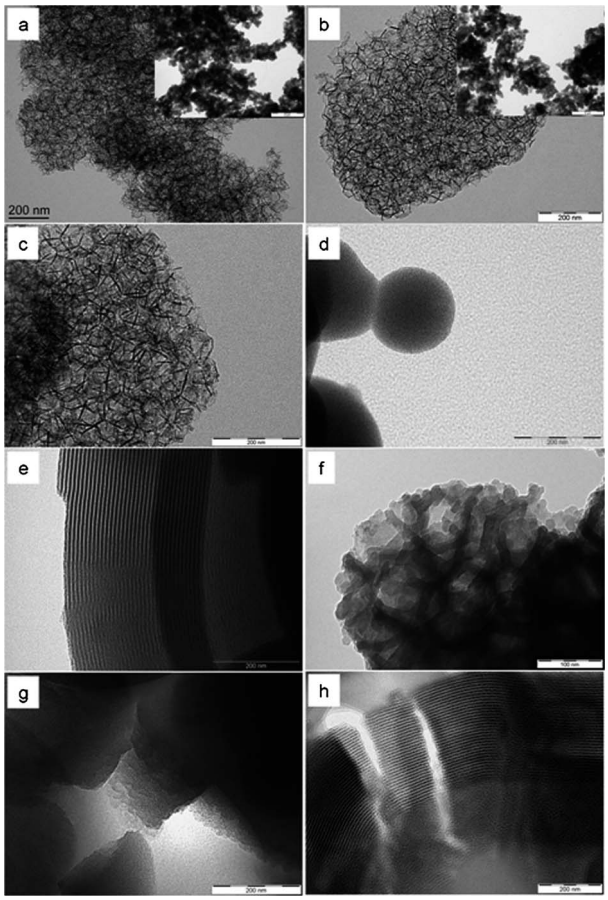

Fig. 2 Transmission electron micrographs of the silica supports and the sorbent composites: (a) as synthesized foam, (b) foam sonicated for 2 h, (c) foam after the steam treatment, (d) MCM-41 mesoporous silica, (e) SBA-15 mesoporous silica, (f) F-PEI423%80, (g) MCM-41PEI423-GDE %80, and (h) SBA-15PEI423-GDE%80. The insets in (a) and (b) are lower magnification images showing the textural structure of the foams (scale bar = 5 μm).

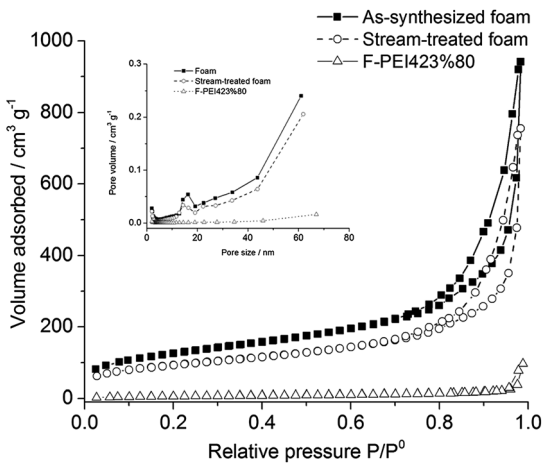

Fig. 3 Nitrogen adsorption–desorption isotherms of the pristine foam, the steam-treated foam, and the PEI-impregnated sorbent F-PEI423%80.

steam-treated foam are 328 $m^2 g^{-1}$ and 1.17 $cm^3 g^{-1}$, respectively. This reduction in surface area and pore volume is in line with mesocellular foams[33] but much less compared to many mesoporous silica supports such as MCM-41 treated under similar conditions.[34] The BET surface area and the pore volume of the amine-impregnated sorbent F-PEI423%80 are much lower (5.2 $m^2 g^{-1}$ and 0.001 $cm^3 g^{-1}$, respectively). The N_2 physisorption results of all systems are summarized in Table S1†. The XRD pattern of the foam shows no diffraction peak (Fig. S1†), which implies that the cells do not possess any significant long-range order, consistent with the morphology seen in the TEM image. No diffraction peak was found in the XRD pattern of the amine-impregnated sorbent either; however, the diffraction intensity is much weaker compared to that of the foam. As the diffraction peak intensity is correlated with the scattering contrast between the silicate walls and the pores,[35–37] Xu *et al.* suggested that the weaker diffraction intensity after PEI impregnation is the result of the amine filling in the mesopores.[6]

The PEI423-impregnated sorbent was further characterized by attenuated total reflectance/Fourier transform infrared (ATR/FTIR) spectroscopy (Fig. S2†). The strong absorption band around 1071 cm^{-1} comes from the Si–O–Si stretching vibrations. Bands at 2931, 2881, 2814, 1454 and 1346 cm^{-1} are due to the CH_2 vibrations of PEI while those at 3300 and 1593 cm^{-1} correspond to the N–H symmetric stretching and bending vibrations, respectively. After CO_2 adsorption, the sorbent shows new absorption bands at 1650, 1548, and 1409 cm^{-1}, which can be assigned to the N–H deformation in RNH_3^+, the C=O stretch, and NCOO skeletal vibrations, respectively,[38] indicative of the formation of carbamates during CO_2 adsorption.

CO_2 adsorption and desorption kinetics of the sorbents

The adsorption kinetics of F-PEI423%80 was gravimetrically evaluated and compared to that of pure PEI423 at 75 °C under 1 atm of 80% CO_2 (balanced with N_2). A sharp weight gain was observed after F-PEI423%80 was exposed to CO_2 (Fig. 4). The corresponding capture capacity was more than 5 mmol g^{-1} after just 5 min. Afterwards, the adsorption continued but at a slower rate. The slow-down can be attributed to the diffusion resistance of CO_2 built up during the adsorption period.[2,6,10,27] A capacity of up to 5.6 mmol g^{-1} was achieved after 60 min, which is among the highest reported for amine-impregnated sorbents under similar conditions.[2] Pure PEI423 exhibited similar two-stage

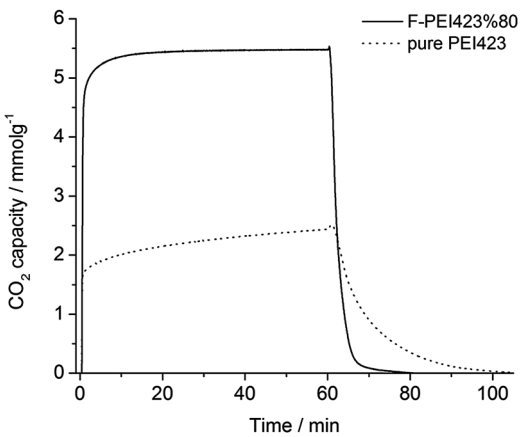

Fig. 4 CO_2 adsorption kinetics of F-PEI423%80 and pure PEI423 under 80% CO_2 and their desorption behaviors under N_2 at 75 °C.

adsorption kinetics. However, its capture capacity in the first adsorption stage was less than 2 mmol g^{-1}. After adsorption for 60 min, the sorbents were regenerated in N_2 at 75 °C. F-PEI423%80 desorbed most of its captured CO_2 in 10 min and was fully regenerated in 20 min. In contrast, PEI423 showed much slower desorption kinetics and took ~40 min to desorb all the CO_2.

Reaction heat of the sorbent

DSC was used to follow the heat evolution during CO_2 adsorption–desorption as described previously.[17] As shown in Fig. 5, the sorbent F-PEI423%80 was first activated under N_2 at 100 °C for 20 min and then cooled down to 40 °C at 10 °C min^{-1}. The associated sensible heat of F-PEI423%80 from 100 to 40 °C is ~21 kJ mol^{-1} (ΔT = 60 °C). During the desorption step using temperature swing (from 75 to 100 °C), the sensible heat is only ~8.5 kJ mol^{-1}, much lower than that of 30% MEA solution (~96 kJ mol^{-1}, ΔT = 40.6 °C).[39] To minimize measurement errors caused by the gas switch and temperature changes, pure CO_2 was used for the adsorption followed by a concentration sweep process for sorbent regeneration. A sharp positive heat flow peak was observed once the sorbent was exposed to CO_2, which is attributed to the exothermic reaction of the impregnated PEI423 with CO_2. The corresponding adsorption heat, ΔH_r, of F-PEI423%80 is 68 kJ mol^{-1}, in the same range as that observed for amine-modified mesoporous silicas (~45 to 95 kJ mol^{-1})[17,39–41] and for sodium aluminosilicate zeolites (~50 to 70 kJ mol^{-1}),[42,43] but higher than that of pure mesoporous silicas, zeolites and metal–organic frameworks that are based mainly on weak physisorption (~30 to 50 kJ mol^{-1}),[40,43,44] indicating that chemisorption is the predominant process in our system. After the purge gas was switched from CO_2 to N_2 at 75 °C, a relatively broad endothermic peak was observed and the related desorption heat is 66 kJ mol^{-1}, slightly lower than the heat required for stripping 30% MEA solution (~72 kJ mol^{-1}).[39] Considering the low sensible heat of F-PEI423%80, the overall energy consumption for F-PEI423%80 (sensible heat plus desorption heat) is much lower than that of 30% MEA solution.

In addition to the DSC measurements, the adsorption heat of F-PEI423%80 was also calculated using the model recently proposed by Ritter *et al.*[45] By assuming that the impregnated amine directly reacts with physisorbed CO_2 that equilibrates with CO_2 in the stream following Henry's law, the CO_2 chemisorption of amine impregnated sorbents can be described by a Langmuir-type adsorption isotherm:[45]

$$\frac{P_{CO_2}}{q_{CO_2}} = \frac{1}{kN} + \frac{1}{N} P_{CO_2} \quad (1)$$

and

$$k = \frac{k_f k_H}{k_b} = k_0 \exp\left(-\frac{\Delta H_r}{RT}\right) \quad (2)$$

where P_{CO2} is the CO_2 partial pressure in the gas stream, q_{CO2} stands for the chemisorbed CO_2 by the impregnated amine, N is the total number of sites available for CO_2, and k, k_f, k_b, and k_H, represent the affinity coefficient between CO_2 and the sorbent, the forward and backward rate constants for the CO_2 chemisorption, and Henry's law constant for physisorbed CO_2, respectively.

The relationship between the CO_2 partial pressure and the sorbent capacity (adsorption for 60 min) is depicted in Fig. 6. The adsorption heat ΔH_r fitted according to eqn (1) is ~43 kJ mol^{-1}, lower than the experimental value measured using DSC (68 kJ mol^{-1}). It is worth noting that k_H was treated as a constant in the model for simplicity (eqn (2)). In fact, as significant diffusion resistance of CO_2 in the impregnated amine develops during the adsorption due to the formation of salt bridges and/or hydrogen-bonded networks of amine-CO_2 zwitterions,[27] the physisorbed CO_2 is less likely to equilibrate fast with CO_2 in the stream, *i.e.* the apparent k_H, and accordingly the resultant affinity coefficient between CO_2 and the sorbent k, tend to be lower than the theoretical value reaching equilibration. As a result, the ΔH_r derived from eqn (1) represents the lower bound for the heat of adsorption.

Stability of the sorbents

Robust long-term sorbent stability and short process cycle time are important to lower cost in practical CO_2 capture applications. While some other novel sorbent regeneration processes have been proposed more recently, to evaluate the long-term stability of the foam-supported amine sorbents, two common

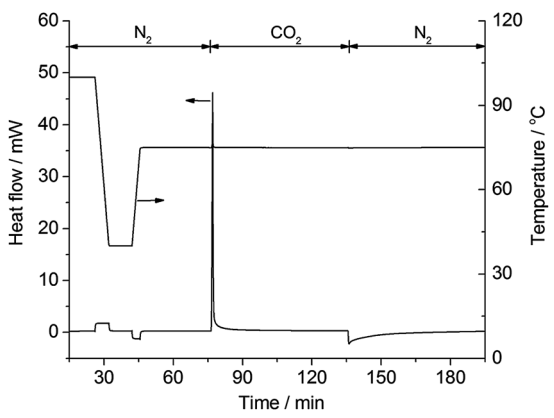

Fig. 5 Representative DSC profile of F-PEI423%80 for CO_2 adsorption under pure CO_2 for 60 min and desorption under N_2 for 60 min at 75 °C.

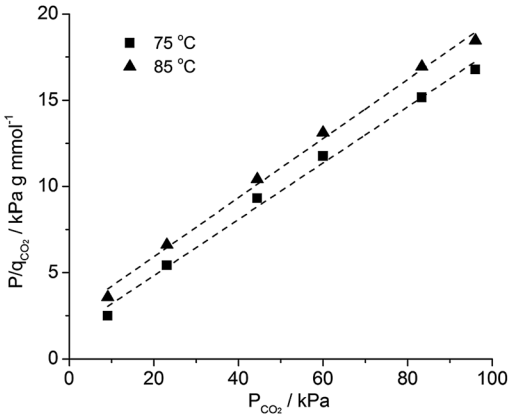

Fig. 6 Relationship between the CO_2 partial pressure and the capacity of F-PEI423%80 (adsorption for 60 min) at different temperatures. The dashed lines are the fits of the model according to eqn (1). R^2 = 0.991.

cyclic adsorption–desorption processes, concentration sweep and temperature swing, were used.[46,47] In order to reduce the cycle time, the activated sorbents were exposed to 80% dry CO_2 (balanced with N_2) at 75 °C only for 10 min due to their rapid adsorption kinetics. Moreover, the nearly linear adsorption kinetics during the adsorption period can simplify the process in practical applications. When concentration sweep was used, the sorbents were regenerated under N_2 at 75 °C for 30 min. In contrast, the sorbents were regenerated under N_2 at 100 °C for 5 min in the temperature swing cycle. As shown in Fig. 7, F-PEI423%80 exhibited good stability using concentration sweep, where the CO_2 capacity dropped only ~7% after 100 cycles at 75 °C. In contrast, the capacity loss was ~29% during temperature cycling. We note that F-PEI423%80 had a weight loss of ~30% after 100 cycles using temperature swing most likely due to the volatilization of amines.

Several groups have investigated the long-term stability of PEI423-impregnated silica sorbents under dry conditions.[45,48–51] Sayari and Belmabkhout examined the stability of PEI-impregnated sorbents (based on pore-expanded MCM-41 mesoporous silicas) using the concentration sweep at different temperatures. A capacity loss of up to 41% was observed after 22 cycles at 105 °C, which was attributed to the formation of urea groups that are ineffective towards CO_2.[48] However, the sorbent capacity dropped by only 14% after 120 cycles at 75 °C,[49] which is consistent with our results here. Ritter *et al.* also showed that porous silica (CARiACT G10 from Fuji Silysia) supported PEI423 sorbent had essentially no capacity loss after 78 concentration sweep cycles at 80 °C.[45] In fact, it has recently been demonstrated that the sorbent degradation under dry CO_2 conditions depends on many factors, such as the nature of amines, the stripping gas and the desorption temperature.[50,51] Sayari *et al.* found that secondary and tertiary amines are more robust than primary amines against urea formation under dry CO_2. Only primary monoamines suffered extensive degradation, when the temperature was below 200 °C.[50] Drage *et al.* systematically studied the stability of PEI-impregnated sorbents under different regeneration conditions and found that using N_2 as a stripping gas the formation of urea was limited, when the cycling temperature was below 130 °C.[51] Since F-PEI423%80 was regenerated under N_2 at desorption temperatures well below 130 °C and PEI423 is dominated by secondary amines, the capacity loss of F-PEI423%80 is more likely due to the volatilization of the impregnated PEI, although the possibility of urea formation cannot be completely ruled out. This assumption was further supported by the difference in cycling performance of F-PEI423%80 and F-PEI10k%80. Because of the use of the high molecular weight PEI ($M_n \approx 10\,000$), F-PEI10k%80 showed almost no weight loss under N_2 at 100 °C for 200 min (Fig. S3†). Similarly, the capacity of F-PEI10k%80 was virtually unchanged after 100 cycles regardless of the regeneration method (temperature swing or concentration sweep) (Fig. 7). Furthermore, both the weight loss of F-PEI423%80 during the temperature swing cycle # 5–22 and the amine loss of the sorbent under N_2 at 100 °C for 200 min were ~9% (Fig. S3†). Their similar capacity degradation (Fig. S4†) further suggests that the capacity loss of F-PEI423%80 is mainly caused by volatilization of the impregnated low molecular weight amine.

In addition to amine volatilization and urea formation, the sorbent performance may gradually degrade due to oxidation and other side reactions under industrially relevant conditions. In a typical setting the sorbents have to be regenerated or replaced once their efficiency drops below a certain point that is practically or economically viable. As a large fraction of the cost of supported amines comes from the supports, their reuse is highly desirable. To evaluate the reuse of the foam support we first washed the amine from the used F-PEI423%80 with ethanol and reimpregnated with fresh PEI. The sorbents using the recycled support showed virtually no change in capture capacity after five washing/reimpregnation cycles compared to that of the virgin sorbent (Fig. S5†).

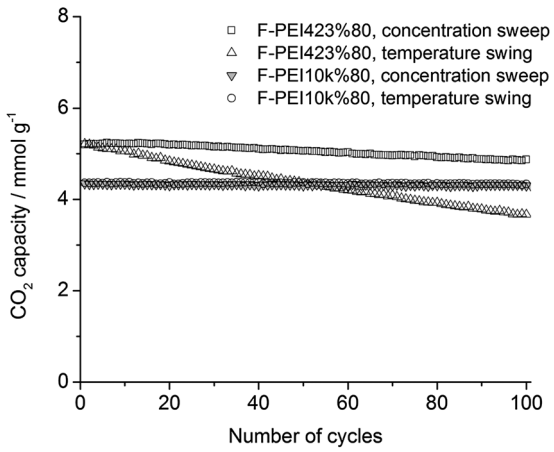

Fig. 7 Cyclic stability of F-PEI423%80 and F-PEI10k%80 using concentration sweep (CO_2 adsorption at 75 °C for 10 min and desorption at 75 °C for 30 min under 1 atm pure N_2) and temperature swing (CO_2 adsorption at 75 °C for 10 min and desorption at 100 °C for 10 min under 1 atm pure N_2).

Relationship between support structure and sorbent capacity

The capacities of the sorbents based on the mesoporous foam were investigated in terms of amine loading and compared with similar sorbents prepared from conventional mesoporous materials (Fig. 8). The capacity of pure PEI was also included for comparison. CO_2 capacities were measured at 75 °C under 1 atm of pure CO_2 for 60 min. The virgin silica foam shows essentially no adsorption of CO_2 under these conditions. The foam-based sorbents show an optimal amine loading at ~80 to 83 wt% with a capacity of ~5.8 mmol g^{-1}, much higher than that of SBA-15-PEI423, MCM-41-PEI423, and pure PEI423. As the N content of PEI423 is ~23.3 mmol N g^{-1}, the stoichiometric ratio of CO_2 to N (CO_2/N) for F-PEI423%80 is 0.31, comparable to that of sorbents based on the textural mesoporous silica,[11] mesocellular foams[21] and mesocapsules,[27] but higher than that of MCM-41-PEI423%75 (CO_2/N = 0.22) and SBA-15-PEI423%75 (CO_2/N = 0.23). In recent contributions Sayari *et al.* reported that coating a layer of long-chain hydrophobic alkyl groups on mesoporous silica can greatly enhance the amine efficiency, up to CO_2/N ≈ 0.36.[49,52] Therefore, we believe it is possible to further improve the sorbent performance of F-PEI with proper surface-functionalization of the foam support.

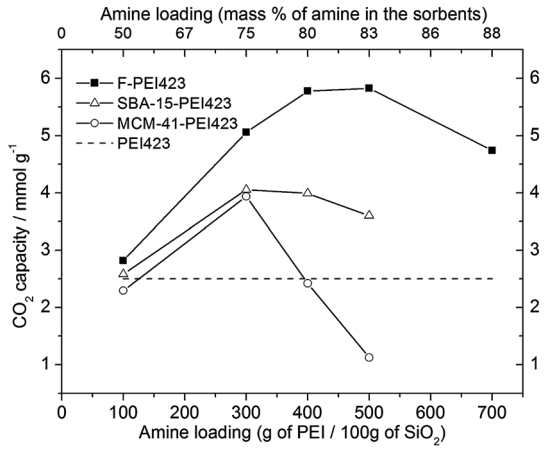

Fig. 8 CO_2 capacity of the sorbents with different amine loadings. The capacity was measured after 60 min at 75 °C under 1 atm of pure CO_2.

As shown experimentally here and in other reports, the structure of the supports significantly affects the capture capacity of supported amine sorbents.[2] Surprisingly, no theoretical understanding of their synergistic relationship has been reported. Here, a simple analysis is presented to rationalize the high efficiency of our new support system and to shed some light on designing optimal support structures.

For amine-impregnated sorbents with relatively high amine loadings, their adsorption is dominated by chemisorption. Under dry CO_2 gas, the stoichiometric ratio of CO_2 to amine (CO_2/N) is typically low, usually <0.3.[2] Therefore, we assume that a stagnant diffusion layer (with a thickness δ) is formed upon the reaction of amine groups with CO_2 and that δ is much thinner than the average thickness of the amine layer in the mesopores. According to eqn (S6) in the ESI†, it is clear that the sorbent capacity n is related amongst other parameters to the effective pore volume of the support $V_{p,e}$ (*i.e.* the maximum space that can be taken by the amine and is accessible to CO_2). Under certain conditions, *e.g.* when ϕ is relatively large and the amine is uniformly coated on the bulk mesoporous supports without any pore blocking ($V_{p,e} \approx V_p$, the total pore volume of the support), the larger the V_p, the higher the theoretical sorbent capacity. Yan *et al.* recently studied amine supported sorbents based on bulk SBA-15 and found that the sorbent capacity did increase with the total pore volume of the support.[18] For sorbents based on hierarchical structures, the adsorption contribution from the external surfaces may not be negligible so that eqn (S1)† becomes too complicated and is beyond the scope of the simple analysis presented here. Nevertheless, this analysis suggests that under certain conditions, larger total pore volume of the support is advantageous and can result in a higher theoretical CO_2 capacity. This prediction is consistent with the experimental results presented in Fig. 8. At the same amine loading, *e.g.* 75 wt% amine, the capture capacity of MCM-41, SBA-15 and the foam based sorbents is 3.8, 4.0 and 5.1 mmol g^{-1}, respectively, which parallels the V_p of MCM-41, SBA-15 and foam-based supports (0.67, 0.89 and 1.46 cm^3 g^{-1}, respectively). The differences in capture capacity become more dramatic as the amine loading increases over 75 wt%. The capture capacities at 83 wt% amine loading are 1.1, 3.5 and 5.8 mmol g^{-1}, respectively for MCM-41, SBA-15, and the foam based sorbents. Beyond a critical amine amount, we suspect that pore blocking dramatically changes the $V_{p,e}$ of the sorbent and thus impedes adsorption.

Conclusion

In summary, a cost-effective silica foam with ultra-large mesopores was developed for high-efficiency supported amine sorbents. The sorbents exhibited fast CO_2 adsorption–desorption kinetics, high adsorption capacity (up to 5.8 mmol g^{-1} under 1 atm of dry CO_2) as well as low energy for sorbent regeneration. The sorbent impregnated with high molecular weight PEI showed good stability over multiple adsorption–desorption cycles. A simple theoretical analysis relating sorbent capacity to the structure of the support is presented and is consistent with the experimental results: under certain adsorption conditions higher support pore volume results in increased sorbent capacity.

Acknowledgements

This publication was based on work supported by Award no. KUS-C1-018-02, made by King Abdullah University of Science and Technology (KAUST).

Notes and references

1 P. M. Cox, R. A. Betts, C. D. Jones, S. A. Spall and I. J. Totterdell, *Nature*, 2000, **408**, 184–187.
2 S. Choi, J. H. Drese and C. W. Jones, *ChemSusChem*, 2009, **2**, 796–854.
3 Q. Wang, J. Luo, Z. Zhong and A. Borgna, *Energy Environ. Sci.*, 2011, **4**, 42–55.
4 D. M. D'Alessandro, B. Smit and J. R. Long, *Angew. Chem., Int. Ed.*, 2010, **49**, 6058–6082.
5 R. Dawson, E. Stöckel, J. R. Holst, D. J. Adams and A. I. Cooper, *Energy Environ. Sci.*, 2011, **4**, 4239–4245.
6 X. C. Xu, C. S. Song, J. M. Andresen, B. G. Miller and A. W. Scaroni, *Energy Fuels*, 2002, **16**, 1463–1469.
7 R. S. Franchi, P. J. E. Harlick and A. Sayari, *Ind. Eng. Chem. Res.*, 2005, **44**, 8007–8013.
8 M. B. Yue, L. B. Sun, Y. Cao, Y. Wang, Z. J. Wang and J. H. Zhu, *Chem.–Eur. J.*, 2008, **14**, 3442–3451.
9 M. B. Yue, Y. Chun, Y. Cao, X. Dong and J. H. Zhu, *Adv. Funct. Mater.*, 2006, **16**, 1717–1722.
10 X. L. Ma, X. X. Wang and C. S. Song, *J. Am. Chem. Soc.*, 2009, **131**, 5777–5783.
11 W. J. Son, J. S. Choi and W. S. Ahn, *Microporous Mesoporous Mater.*, 2008, **113**, 31–40.
12 A. Heydari-Gorji, Y. Yang and A. Sayari, *Energy Fuels*, 2011, **25**, 4206–4210.
13 R. Sanz, G. Calleja, A. Arencibia and E. S. Sanz-Perez, *Appl. Surf. Sci.*, 2010, **256**, 5323–5328.
14 X. W. Liu, L. Zhou, X. Fu, Y. Sun, W. Su and Y. P. Zhou, *Chem. Eng. Sci.*, 2007, **62**, 1101–1110.
15 X. C. Xu, C. S. Song, J. M. Andresen, B. G. Miller and A. W. Scaroni, *Microporous Mesoporous Mater.*, 2003, **62**, 29–45.
16 A. N. M. Peeters, A. P. C. Faaij and W. C. Turkenburg, *Int. J. Greenhouse Gas Control*, 2007, **1**, 396–417.
17 M. L. Gray, J. S. Hoffman, D. C. Hreha, D. J. Fauth, S. W. Hedges, K. J. Champagne and H. W. Pennline, *Energy Fuels*, 2009, **23**, 4840–4844.
18 X. L. Yan, L. Zhang, Y. Zhang, G. D. Yang and Z. F. Yan, *Ind. Eng. Chem. Res.*, 2011, **50**, 3220–3226.
19 V. Zelenak, M. Badanicova, D. Halamova, J. Cejka, A. Zukal, N. Murafa and G. Goerigk, *Chem. Eng. J.*, 2008, **144**, 336–342.
20 G. Qi, L. Fu, X. Duan, B. H. Choi, M. Abraham and E. P. Giannelis, *Greenhouse Gases: Sci. Technol.*, 2011, **1**, 278–284.
21 X. L. Yan, L. Zhang, Y. Zhang, K. Qiao, Z. F. Yan and S. Komarneni, *Chem. Eng. J.*, 2011, **168**, 918–924.

22 S. H. Liu, C. H. Wu, H. K. Lee and S. B. Liu, *Top. Catal.*, 2010, **53**, 210–217.
23 D. J. N. Subagyono, Z. Liang, G. P. Knowles and A. Chaffee, *Chem. Eng. Res. Des.*, 2011, **89**, 1647–1657.
24 C. Chen, W. J. Son, K. S. You, J. W. Ahn and W. S. Ahn, *Chem. Eng. J.*, 2010, **161**, 46–52.
25 C. Chen, S. T. Yang, W. S. Ahn and R. Ryoo, *Chem. Commun.*, 2009, 3627–3629.
26 G. Qi, Y. Wang, L. Estevez, A. Switzer, X. Duan, Y. Yang and E. P. Giannelis, *Chem. Mater.*, 2010, **22**, 2693–2695.
27 G. G. Qi, Y. B. Wang, L. Estevez, X. N. Duan, N. Anako, A. H. A. Park, W. Li, C. W. Jones and E. P. Giannelis, *Energy Environ. Sci.*, 2011, **4**, 444–452.
28 W. Li, P. Bollini, S. A. Didas, S. Choi, J. H. Drese and C. W. Jones, *ACS Appl. Mater. Interfaces*, 2010, **2**, 3363–3372.
29 D. Y. Zhao, J. L. Feng, Q. S. Huo, N. Melosh, G. H. Fredrickson, B. F. Chmelka and G. D. Stucky, *Science*, 1998, **279**, 548–552.
30 W. W. Lukens, P. D. Yang and G. D. Stucky, *Chem. Mater.*, 2001, **13**, 28–34.
31 P. Schmidt-Winkel, W. W. Lukens, D. Y. Zhao, P. D. Yang, B. F. Chmelka and G. D. Stucky, *J. Am. Chem. Soc.*, 1999, **121**, 254–255.
32 S. S. Kim, T. R. Pauly and T. J. Pinnavaia, *Chem. Commun.*, 2000, 1661–1662.
33 W. Li, P. Bollini, S. A. Didas, S. Choi, J. H. Drese and C. W. Jones, *ACS Appl. Mater. Interfaces*, 2010, **2**, 3363–3372.
34 K. Cassiers, T. Linssen, M. Mathieu, M. Benjelloun, K. Schrijnemakers, P. Van Der Voort, P. Cool and E. Vansant, *Chem. Mater.*, 2002, **14**, 2317–2324.
35 B. Marler, U. Oberhagemann, S. Vortmann and H. Gies, *Microporous Mater.*, 1996, **6**, 375–383.
36 W. Hammond, E. Prouzet, S. D. Mahanti and T. J. Pinnavaia, *Microporous Mesoporous Mater.*, 1999, **27**, 19–25.
37 J. Sauer, F. Marlow and F. Schuth, *Phys. Chem. Chem. Phys.*, 2001, **3**, 5579–5584.
38 X. X. Wang, V. Schwartz, J. C. Clark, X. L. Ma, S. H. Overbury, X. C. Xu and C. S. Song, *J. Phys. Chem. C*, 2009, **113**, 7260–7268.
39 F. S. Su, C. S. Lu and H. S. Chen, *Langmuir*, 2011, **27**, 8090–8098.
40 M. R. Mello, D. Phanon, G. Q. Silveira, P. L. Llewellyn and C. M. Ronconi, *Microporous Mesoporous Mater.*, 2011, **143**, 174–179.
41 G. Knowles, J. Graham, S. Delaney and A. Chaffee, *Fuel Process. Technol.*, 2005, **86**, 1435–1448.
42 J. A. Dunne, M. Rao, S. Sircar, R. J. Gorte and A. L. Myers, *Langmuir*, 1996, **12**, 5896–5904.
43 R. V. Siriwardane, M. S. Shen and E. P. Fisher, *Energy Fuels*, 2005, **19**, 1153–1159.
44 S. Bourrelly, P. L. Llewellyn, C. Serre, F. Millange, T. Loiseau and G. Ferey, *J. Am. Chem. Soc.*, 2005, **127**, 13519–13521.
45 A. D. Ebner, M. L. Gray, N. G. Chisholm, Q. T. Black, D. D. Mumford, M. A. Nicholson and J. A. Ritter, *Ind. Eng. Chem. Res.*, 2011, **50**, 5634–5641.
46 W. Li, S. Choi, J. H. Drese, M. Hornbostel, G. Krishnan, P. M. Eisenberger and C. W. Jones, *ChemSusChem*, 2010, **3**, 899–903.
47 J. A. Wurzbacher, C. Gebald and A. Steinfeld, *Energy Environ. Sci.*, 2011, **4**, 3584–3592.
48 A. Sayari and Y. Belmabkhout, *J. Am. Chem. Soc.*, 2010, **132**, 6312–6314.
49 A. Heydari-Gorji, Y. Belmabkhout and A. Sayari, *Langmuir*, 2011, **27**, 12411–12416.
50 A. Sayari, Y. Belmabkhout and E. Da'na, *Langmuir*, 2012, **28**, 4241–4247.
51 T. C. Drage, A. Arenillas, K. M. Smith and C. E. Snape, *Microporous Mesoporous Mater.*, 2008, **116**, 504–512.
52 A. Heydari-Gorji and A. Sayari, *Chem. Eng. J.*, 2011, **173**, 72–79.